HHS Public Access

Author manuscript

NMR Biomed. Author manuscript; available in PMC 2017 January 01.

Published in final edited form as:

NMR Biomed. 2016 January ; 29(1): 84–89. doi:10.1002/nbm.3442.

Initial Evaluation of Hepatic T_1 Relaxation Time as an Imaging Marker of Liver Disease Associated with Autosomal Recessive Polycystic Kidney Disease (ARPKD)

Ying Gao[1], **Bernadette O. Erokwu**[2], **David A. DeSantis**[3], **Colleen M. Croniger**[3], **Rebecca M. Schur**[1], **Lan Lu**[2,4], **Jose Mariappuram**[5], **Katherine M. Dell**[5,6,7], and **Chris A. Flask**[1,2,7,*]

[1]Department of Biomedical Engineering, Case Western Reserve University, Cleveland, Ohio, United States of America

[2]Department of Radiology, Case Western Reserve University, Cleveland, Ohio, United States of America

[3]Department of Nutrition, Case Western Reserve University, Cleveland, Ohio, United States of America

[4]Department of Urology, Case Western Reserve University, Cleveland, Ohio, United States of America

[5]CWRU Center for the Study of Kidney Disease and Biology, MetroHealth Campus, Case Western Reserve University, Cleveland, Ohio, United States of America

[6]Cleveland Clinic Children's, Cleveland, Ohio, United States of America

[7]Department of Pediatrics, Case Western Reserve University, Cleveland, Ohio, United States of America

Abstract

Autosomal Recessive Polycystic Kidney Disease (ARPKD) is a potentially lethal multi-organ disease affecting both the kidneys and the liver. Unfortunately, there are currently no non-invasive methods to monitor liver disease progression in ARPKD patients, limiting the study of potential therapeutic interventions. Herein, we performed an initial investigation of T_1 relaxation time as a potential imaging biomarker to quantitatively assess the two primary pathologic hallmarks of ARPKD liver disease: biliary dilatation and periportal fibrosis in the PCK rat model of ARPKD. T_1 relaxation time results were obtained for five PCK rats at 3 months of age using a Look-Locker acquisition on a Bruker Biospec 7.0 T MRI scanner. Six 3-month-old Sprague-Dawley (SD) rats were also scanned as controls. All animals were euthanized after the 3-month scans for histological and biochemical assessments of bile duct dilatation and hepatic fibrosis for comparison. PCK rats exhibited significantly increased liver T_1 values (mean±standard deviation = 935±39 ms) compared to age-matched SD control rats (847±26 ms, $p = 0.01$). One PCK rat exhibited severe cholangitis (mean T_1 = 1413 ms), which occurs periodically in ARPKD patients. The observed increase in the *in vivo* liver T_1 relaxation time correlated significantly with three

*Corresponding author: Chris A. Flask, PhD, Associate Professor of Radiology, 11100 Euclid Ave / Bolwell B115, Cleveland, OH 44106, 216-844-4963, caf@case.edu.

histological and biochemical indicators of biliary dilatation and fibrosis: bile duct area percent (R=0.85, p=0.002), periportal fibrosis area percent (R=0.82, p=0.004) and hydroxyproline content (R=0.76, p=0.01). These results suggest that hepatic T_1 relaxation time may provide a sensitive and non-invasive imaging biomarker to monitor ARPKD liver disease.

Keywords

Autosomal Recessive Polycystic Kidney Disease (ARPKD); T1; FISP; high-field MRI; liver disease; biliary dilatation; fibrosis

INTRODUCTION

Autosomal Recessive Polycystic Kidney Disease (ARPKD) is an inherited disease that affects approximately 1/20,000 children in all ethnic groups, and is clinically and histologically distinct from Autosomal Dominant PKD (ADPKD) (1). Fundamentally, ARPKD is a multi-organ disease characterized by both progressive kidney and liver disease. ARPKD kidney disease is characterized by markedly enlarged kidneys with diffuse microscopic collecting duct cysts, usually evident at birth. Approximately 40% of patients develop kidney failure by age 15 (2). ARPKD liver disease is a developmental biliary tract disease characterized by progressive bile duct proliferation and dilatation and dense periportal fibrosis. It is present histologically in all ARPKD patients at birth, but may not be clinically evident until later childhood or early adulthood (3). Importantly, clinically-significant ARPKD liver disease is becoming more prevalent as more patients survive into adulthood following kidney transplantation (4,5).

Unfortunately, there are currently no clinically available, disease-specific therapies for ARPKD liver disease and, therefore, treatment is limited to medical or surgical management of complications. Although some novel therapies have shown promise in the PCK rat model of ARPKD (6,7), clinical trials of these therapeutics in ARPKD patients have not been possible due to the lack of established methods to safely and accurately monitoring liver disease progression. Liver biopsies are invasive and conventional biochemical clinical measures of liver/biliary tract disease (e.g., serum bilirubin, liver enzymes, serum albumin, gamma-glutamyl transferase), are typically normal until the disease is more advanced (3,8). Alternatively, imaging methodologies, including ultrasound-based elastography, magnetic resonance elastography, and contrast-enhanced MRI techniques (such as delayed enhancement MRI), have been used successfully in adults and children to assess liver cirrhosis, predict the presence of esophageal varices, assess hepatic perfusion, and screen for the presence of liver fibrosis in at risk patients (9–14). However, these methodologies have several significant limitations in terms of quantitating the severity of liver disease in ARPKD patients. First, because it is exclusively a fibrocystic biliary tract disease, there is minimal hepatocyte involvement and overt cirrhosis is a very late finding. Second, gadolinium-based contrast studies are not appropriate in ARPKD patients due to concerns about the life-threatening toxicities that can occur from gadolinium chelates in patients with chronic kidney disease (15). Finally, several of these methodologies require specialized equipment and operator expertise that may not be available in many clinical practices.

Therefore, a more sensitive, clinically-available, non-invasive marker for assessing liver disease is urgently needed for pediatric and adult ARPKD patients.

As described above, one of the key aspects of ARPKD liver disease is increased biliary proliferation and dilatation. Importantly, and in contrast to other more common forms of hepatic fibrosis, the biliary proliferation and dilatation observed in ARPKD liver disease is pathophysiologically linked to periportal fibrosis (8). As the T_1 and T_2 relaxation times for bile is significantly higher than liver parenchyma, we hypothesized that MRI relaxometry assessments could be used to provide a straightforward assessment of ARPKD liver disease.

In this initial study, we evaluated the capability of T_1 MRI to detect liver disease in the PCK rat model of ARPKD (16–18). *In vivo* T_1 relaxometry data were obtained for groups of PCK rats and Sprague-Dawley (SD) control rats at 3 months of age. The T_1 data were acquired using a Fast Imaging with Steady-state free Precession (FISP)-based Look-Locker technique that provides T_1-weighted images with minimal artifacts on high field MRI scanners (19). The T_1 MRI findings were then compared with three histologic and biochemical assays of biliary dilatation and fibrosis for validation.

METHODS

All animal experiments were conducted according to approved Institutional Animal Care and Use Committee protocols at Case Western Reserve University.

Animal models

T_1 relaxation time assessments were obtained for cohorts of male PCK (n=5) and SD control (n=6) rats at 3 months of age. The PCK rat is a model of human ARPKD, which spontaneously arose in a Sprague Dawley colony. PCK rats harbor a mutation in the rat orthologue of *PKHD1*, the human gene that encodes fibrocystin. PCK rats develop progressive cystic renal disease as well as biliary dilatation and periportal fibrosis that is consistent with human ARPKD liver disease (16,17). PCK liver disease is evident histologically within a week after birth and becomes severe by 6–7 months of age. A subset of animals develop chronic ascending cholangitis (biliary duct infection) and exhibit more severe, progressive liver disease, which can also occur in humans (20,21). All animals were purchased from Charles River Laboratories and were provided with standard rodent chow and water ad libitum. PCK rats and SD rats were scanned at 3 months of age to enable imaging and histological comparisons of PCK rats with normal controls.

MRI experiments

In vivo MRI experiments were conducted on a 7.0 T Bruker Biospec small animal MRI scanner (Bruker Inc., Billerica, MA). Each animal was initially anesthetized with 2–3% isoflurane in oxygen and positioned with its liver at isocenter in a 72-mm cylindrical transmit / receive volume coil to ensure uniform radiofrequency excitation. Animals were provided with 1–3% isoflurane anesthesia continuously throughout the imaging procedure via a nosecone. An animal monitoring and control system (SA Instruments, Stony Brook, NY) was used to maintain each animal's respiration rate (40–60 breaths / minute) and core body temperature (35 ± 1°C).

High resolution, axial T_2-weighted images were acquired with a multi-echo spin echo acquisition (TR=2000ms, TE=8ms, spatial resolution = 0.312mm × 0.312mm × 2mm, number of echoes per excitation=8) (22). A central region of the liver was selected to limit partial volume effects of the lungs and the gastrointestinal tract, respectively. T_1 relaxation time data were acquired with a FISP-based Look-Locker acquisition to limit the image artifacts as well as the effects of noise on the liver T_1 assessments (19,23). Briefly, this method combines an initial non-selective Hermite inversion pulse, followed by 8 continuous and sequential FISP image repetitions (linear encoding; single slice; slice thickness, 1.5 mm; matrix, 256 × 256; field of view, 6 cm × 6 cm; spatial resolution, 0.234 mm × 0.234 mm × 1.5 mm; tip angle, 10°; TR/TE = 3.233/1.616ms; 827.6 ms/image; inversion preparation time = 6.5 ms). Sampling points in the relaxation curve were the time points when the center of k space of the 8 images were acquired (TI = 420 ms, 1248 ms, 2076 ms, 2903 ms, 3731 ms, 4559 ms, 5386 ms, and 6214 ms, respectively). An additional delay of ~13 seconds was implemented between successive averages to allow for full relaxation of the magnetization between averages, thus avoiding systematic errors in T_1 estimation and to reduce the gradient duty cycle. A total of 50 averages were acquired over a total acquisition time of 16 minutes and 40 seconds to further limit the effects of noise on the liver T_1 data. Respiratory triggering was also applied before the inversion pulse to limit respiratory motion artifacts. Voxel-wise T_1 relaxation maps were calculated using previously described methods (24,25):

$$M_z(TI)=A-B\,exp(-TI/C) \quad [1]$$

where $A = M_0(T_1^*/T_1)$, $B = M_0(1+T_1^*/T_1)$, $C = T_1^*$, M_z is the longitudinal magnetization, TI is the inversion time, M_0 is the equilibrium magnetization, and T_1^* is the effective relaxation time. A, B and C were obtained with a least-squares error fit to the three-parameter model. T_1 values were then calculated by the following equation:

$$T_1=C(B/A-1) \quad [2]$$

A region of interest (ROI) was manually selected for each animal covering a large portion of the liver to calculate the mean liver T_1 value for each animal. Large blood vessels were avoided in the ROI analysis to limit the effects of vasculature on the T_1 relaxation time analysis.

Histological and biochemical analyses

At the completion of the imaging study, animals were euthanized and tissue was collected for histopathologic and biochemical assessments. A portion of the left lateral lobe of the liver was excised and fixed in 4% paraformaldehyde and embedded in paraffin as described previously (16). Liver sections (7μm) were stained with Masson's Trichrome (Richard Allan Scientific, Waltham, MA) for detection of collagen. The percentage of collagen staining (for fibrosis assessments) and biliary duct area (for biliary dilatation assessment) were obtained by pixel counting and expressed as the percent of total liver parenchyma. Biochemical hydroxyproline assessments were also performed on the liver specimens, as described in the previous study (26). Cholangitis was identified by visual inspection of the histologic sections for evidence of purulent material or inflammatory cells within the bile ducts (20).

Statistical analyses

Means and standard deviations (std) of the liver T_1 results for the PCK and SD control rats were calculated for each group as a whole. Unpaired 2-tailed Student's *t*-tests were used to compare the liver T_1 results between the two groups. A Pearson correlation coefficient was used to compare the liver T_1 relaxation findings from the PCK and SD rats with the quantitative fibrosis scores, bile duct area and hydroxyproline assessments. A *p*-value of less than 0.05 was considered significant for both the Student's *t*-tests as well as the Pearson correlation coefficients.

RESULTS

Comparison of T_1 relaxation in PCK and SD control rats

Representative liver images from the Look-Locker acquisition as well as the final T_1 relaxation time maps from a 3-month-old SD control rat (top panel) and two 3-month-old PCK rats (middle and bottom panels) are shown in Figure 1. Among the five PCK rats studied, we observed from histology that one of the PCK rats suffered from cholangitis (bottom panel) which mirrors the variation in liver disease severity observed in ARPKD patients. Representative T_1-weighted images at inversion times of 420 ms, 1248 ms, 2076 ms and 6214 ms for the three rats are shown in **columns a-d** in Figure 1, respectively. The liver T_1 maps (**column e**) for the PCK rat (middle row) show increased hepatic T_1 values in comparison to the SD control rat (top row). The PCK rat with severe cholangitis (bottom row) exhibited extensive regions with increased T_1 relaxation time values consistent with biliary cysts observed in some ARPKD patients with more severe liver disease.

Mean liver T_1 values for the cohorts of SD and PCK rats are shown in Figure 2. Excluding the severe PCK rat with cholangitis from the analysis (T_1 = 1413 ms), the group of PCK rats (n=4) still exhibited a significantly higher mean T_1 relaxation estimation (mean ± std = 935±39 ms, p = 0.01) when compared with the SD control rats (n=6, mean ± std = 847±26 ms).

Comparison of *in vivo* liver T_1 relaxation time with histological and biochemical assessments of biliary dilatation and hepatic fibrosis

Photomicrographs of Masson's Trichrome-stained liver sections from a 3-month-old control SD rat and two 3-month-old PCK rats are shown in Figure 3. The PCK rats show increased regions of fibrosis (blue regions staining collagen) around dilated bile ducts (white regions with asterisks) in comparison to the SD rat. It should be noted that the PCK rat with cholangitis exhibited more extensive fibrosis staining and increased bile duct dilatation than both the more typical PCK rat and the SD control rat as previously described in this model (27). The relationship of mean hepatic T_1 relaxation time to bile duct area percent, fibrosis area percent, and hydroxyproline content (μg / mg protein) for each rat (excluding the PCK rat with cholangitis) is shown in Figures 4a-c, respectively. Importantly, all three indicators: bile duct area percent (R=0.85, p=0.002), trichrome fibrosis scores (R=0.82, p=0.004) and hydroxyproline content (R=0.76, p=0.01) demonstrated a significant correlation with the mean *in vivo* liver T_1 relaxation assessments.

DISCUSSION

In this initial study, we have shown that quantitative T_1 relaxation time assessments of the liver in PCK rats can provide a non-invasive and quantitative assessment of ARPKD liver disease. Specifically, the FISP-based Look-Locker technique demonstrated statistically significant increases in hepatic T_1 relaxation time in PCK rats in comparison to SD control rats at 3 months of age. Importantly, these hepatic T_1 relaxometry assessments resulted in significant correlations with both histologic scores of biliary dilatation and hepatic fibrosis as well as biochemical hydroxyproline content assessing hepatic collagen content. As there are currently no clinical gold standard assessments for ARPKD liver disease, this study suggests that evaluation of T_1 relaxation time is a safe and sensitive imaging biomarker for this rare, but potentially lethal pediatric disease.

The presented results are significant from multiple aspects. First, the significantly increased liver T_1 estimation observed in PCK rats in comparison to SD controls (Figure 2) suggests the increased T_1 relaxation time can detect ARPKD liver disease. Further, the link between T_1 and the pathophysiologic changes associated with ARPKD liver disease is supported by the findings that T_1 correlates significantly with the primary pathologic hallmarks of disease severity: biliary dilatation and hepatic (periportal) fibrosis. In addition, although not thoroughly studied in this initial investigation, the T_1 relaxation time appears to be impacted by cholangitis observed in the single PCK rat (Figure 1), which occurs intermittently in ARPKD patients. Altogether, these *in vivo* results suggest that quantitative T_1 relaxation time assessments can provide a non-invasive measure of ARPKD liver disease severity.

The T_1 relaxometric assessment offers multiple specific advantages for the assessment of ARPKD liver disease. First, this simple T_1 measurement is entirely non-invasive and requires no exogenous contrast agents. This method limits the risks of other methodologies to assess liver disease, such as bleeding complications associated with biopsies or toxicities resulting from gadolinium-based MRI imaging contrast agents in patients with chronic kidney disease. This is extremely important for eventual use in ARPKD patients as ARPKD includes both progressive kidney and liver disease components (3,4). In addition, while other techniques such as MR Elastography (MRE) and ultrasound have gained significant momentum in recent years for the assessment of hepatic fibrosis (28,29), T_1 relaxation time assessments are already available on virtually all modern MRI scanners offering the potential for rapid dissemination for routine clinical use. The FISP-based acquisition itself also offers reduced image artifacts, especially on high field MRI scanners, in comparison to echo-planar imaging (EPI) and True FISP (19). It is worth noting that the FISP acquisition provides additional T_2 weighting in the Look-Locker images in comparison to the previously described spoiled gradient echo acquisitions. However, this impact is partially ameliorated by the small tip angle. In this initial preclinical MRI study, 50 averages were acquired over ~16 min for a single imaging slice to obtain high quality T_1 relaxation assessments. However, Look-Locker and other previously described T_1 relaxation time assessments have already been implemented on lower field human MRI systems to provide quantitative imaging assessments in a single breathhold (30,31). Therefore, T_1 relaxometric assessments could provide a safe and effective tool for longitudinal studies in infant and pediatric ARPKD patients.

This initial preclinical imaging study had several important limitations and opportunities for future study. The PCK and SD control rats were evaluated only at a single time point (3 months of age), when disease is evident histologically. What remains to be determined is if the T_1 relaxation time assessments are sensitive enough to: 1) detect very early-stage ARPKD liver disease (PCK rats at approximately 1 month of age); and 2) monitor liver disease progression over time. As such, additional imaging studies are needed to track liver disease progression in PCK rats over the full course of the disease progression from 1 to 6 months of age. In addition, in this study, we did not perform any comparison with alternative quantitative MRI techniques, which may also be useful in detecting biliary dilatation / hepatic fibrosis. As bile is known to have increased T_1 and T_2 relaxation times relative to liver parenchyma (32,33), T_2 relaxometric assessments may also provide a direct measure of biliary dilatation / proliferation. Other techniques such as Magnetization Transfer and Diffusion MRI assessments may also provide additional information on ARPKD liver disease (34,35). While these various techniques offer specific advantages and disadvantages for both preclinical and future clinical studies, a thorough comparison of these methods was beyond the scope of this initial preclinical and histological evaluation.

In conclusion, we have performed an initial preclinical study to demonstrate that T_1 relaxation time can detect liver disease in the orthologous PCK rat model of ARPKD. We have shown that the straightforward, non-contrast, readily-translatable FISP-based Look-Locker technique can sensitively identify increased liver T_1 relaxation in PCK rats in comparison to SD controls and distinguished a PCK rat with cholangitis from other PCK rats not similarly infected. In addition, these liver T_1 assessments correlated significantly with two gold-standard histopathologic assessments of hepatic fibrosis and with histologic assessments of biliary dilatation. These initial imaging results, therefore, suggest that T_1 relaxation time may provide a useful imaging marker to not only detect ARPKD liver disease, assess severity, and to monitor disease progression.

Acknowledgements

The authors would like to acknowledge the support of NIH/NIDDK RO1 DK085099, NIH/NIDDK K12 DK100014, the Case Comprehensive Cancer Center (NIH/NCI P30 CA43703), and the Clinical and Translation Science Collaborative of Cleveland (NIH/NCATS UL1 TR000439) and the technical support and liver disease expertise from Dr. Rebecca G. Wells, M.D.

Abbreviations used

ARPKD	autosomal recessive polycystic kidney disease
std	standard deviation
FISP	fast imaging with steady-state free precession
SD	Sprague-Dawley
ROI	region of interest
EPI	echo-planar imaging

REFERENCES

1. Dell KM. The spectrum of polycystic kidney disease in children. Adv. Chronic Kidney Dis. 2011; 18(5):339–347. [PubMed: 21896375]
2. Roy S, Dillon MJ, Trompeter RS, Barratt TM. Autosomal recessive polycystic kidney disease: long-term outcome of neonatal survivors. Pediatr. Nephrol. 1997; 11(3):302–306. [PubMed: 9203177]
3. Shneider BL, Magid MS. Liver disease in autosomal recessive polycystic kidney disease. Pediatr. Transplant. 2005; 9(5):634–639. [PubMed: 16176423]
4. Guay-Woodford LM, Desmond RA. Autosomal recessive polycystic kidney disease: the clinical experience in North America. Pediatrics. 2003; 111(5 Pt 1):1072–1080. [PubMed: 12728091]
5. Davis ID, Ho M, Hupertz V, Avner ED. Survival of childhood polycystic kidney disease following renal transplantation: the impact of advanced hepatobiliary disease. Pediatr. Transplant. 2003; 7(5): 364–369. [PubMed: 14738296]
6. Masyuk TV, Masyuk AI, Torres VE, Harris PC, Larusso NF. Octreotide inhibits hepatic cystogenesis in a rodent model of polycystic liver disease by reducing cholangiocyte adenosine 3', 5'-cyclic monophosphate. Gastroenterology. 2007; 132(3):1104–1116. [PubMed: 17383431]
7. Masyuk TV, Radtke BN, Stroope AJ, Banales JM, Gradilone SA, Huang B, Masyuk AI, Hogan MC, Torres VE, Larusso NF. Pasireotide is more effective than octreotide in reducing hepatorenal cystogenesis in rodents with polycystic kidney and liver diseases. Hepatology. 2013; 58(1):409–421. [PubMed: 23172758]
8. Kamath BM, Piccoli DA. Heritable disorders of the bile ducts. Gastroenterol. Clin. North Am. 2003; 32(3):857–875. vi. [PubMed: 14562578]
9. van Rijn RR, Nievelstein RA. Paediatric ultrasonography of the liver, hepatobiliary tract and pancreas. Eur. J. Radiol. 2014; 83(9):1570–1581. [PubMed: 24780818]
10. Stenzel M, Mentzel HJ. Ultrasound elastography and contrast-enhanced ultrasound in infants, children and adolescents. Eur. J. Radiol. 2014; 83(9):1560–1569. [PubMed: 25022978]
11. Serai SD, Wallihan DB, Venkatesh SK, Ehman RL, Campbell KM, Sticka J, Marino BS, Podberesky DJ. Magnetic resonance elastography of the liver in patients status-post fontan procedure: feasibility and preliminary results. Congenit. Heart Dis. 2014; 9(1):7–14. [PubMed: 24134059]
12. Poynard T, de Ledinghen V, Zarski JP, Stanciu C, Munteanu M, Vergniol J, France J, Trifan A, Le Naour G, Vaillant JC, Ratziu V, Charlotte F. Relative performances of FibroTest, Fibroscan, and biopsy for the assessment of the stage of liver fibrosis in patients with chronic hepatitis C: a step toward the truth in the absence of a gold standard. J. Hepatol. 2012; 56(3):541–548. [PubMed: 21889468]
13. Alisi A, Pinzani M, Nobili V. Diagnostic power of fibroscan in predicting liver fibrosis in nonalcoholic fatty liver disease. Hepatology. 2009; 50(6):2048–2049. [PubMed: 19937689]
14. Aronhime S, Calcagno C, Jajamovich GH, Dyvorne HA, Robson P, Dieterich D, Fiel MI, Martel-Laferriere V, Chatterji M, Rusinek H, Taouli B. DCE-MRI of the liver: effect of linear and nonlinear conversions on hepatic perfusion quantification and reproducibility. J. Magn. Reson. Imaging. 2014; 40(1):90–98. [PubMed: 24923476]
15. Saab G, Abu-Alfa A. Nephrogenic systemic fibrosis--implications for nephrologists. Eur. J. Radiol. 2008; 66(2):208–212. [PubMed: 18342470]
16. Goto M, Hoxha N, Osman R, Wen J, Wells RG, Dell KM. Renin-angiotensin system activation in congenital hepatic fibrosis in the PCK rat model of autosomal recessive polycystic kidney disease. J. Pediatr. Gastroenterol. Nutr. 2010; 50(6):639–644. [PubMed: 20400910]
17. Masyuk TV, Huang BQ, Masyuk AI, Ritman EL, Torres VE, Wang X, Harris PC, Larusso NF. Biliary dysgenesis in the PCK rat, an orthologous model of autosomal recessive polycystic kidney disease. Am. J. Pathol. 2004; 165(5):1719–1730. [PubMed: 15509540]
18. Masyuk TV, Huang BQ, Ward CJ, Masyuk AI, Yuan D, Splinter PL, Punyashthiti R, Ritman EL, Torres VE, Harris PC, LaRusso NF. Defects in cholangiocyte fibrocystin expression and ciliary structure in the PCK rat. Gastroenterology. 2003; 125(5):1303–1310. [PubMed: 14598246]
19. Gao Y, Goodnough CL, Erokwu BO, Farr GW, Darrah R, Lu L, Dell KM, Yu X, Flask CA. Arterial spin labeling-fast imaging with steady-state free precession (ASL-FISP): a rapid and

quantitative perfusion technique for high-field MRI. NMR Biomed. 2014; 27(8):996–1004. [PubMed: 24891124]

20. Sanzen T, Harada K, Yasoshima M, Kawamura Y, Ishibashi M, Nakanuma Y. Polycystic kidney rat is a novel animal model of Caroli's disease associated with congenital hepatic fibrosis. Am. J. Pathol. 2001; 158(5):1605–1612. [PubMed: 11337358]
21. Hoyer PF. Clinical manifestations of autosomal recessive polycystic kidney disease. Curr. Opin. Pediatr. 2015; 27(2):186–192. [PubMed: 25689455]
22. Hennig J, Nauerth A, Friedburg H. RARE imaging: a fast imaging method for clinical MR. Magn. Reson. Med. 1986; 3(6):823–833. [PubMed: 3821461]
23. Goodnough CL, Gao Y, Li X, Qutaish MQ, Goodnough LH, Molter J, Wilson D, Flask CA, Yu X. Lack of dystrophin results in abnormal cerebral diffusion and perfusion in vivo. Neuroimage. 2014; 102:809–816. [PubMed: 25213753]
24. Deichmann R, Haase A. Quantification of T_1 Values by Snapshot-Flash NMR Imaging. J. Magn. Reson. 1992; 96(3):608–612.
25. Jakob PM, Hillenbrand CM, Wang TT, Schultz G, Hahn D, Haase A. Rapid quantitative lung ^1H T_1 mapping. J. Magn. Reson. Imaging. 2001; 14(6):795–799. [PubMed: 11747038]
26. Reddy GK, Enwemeka CS. A simplified method for the analysis of hydroxyproline in biological tissues. Clin. Biochem. 1996; 29(3):225–229. [PubMed: 8740508]
27. Ren XS, Sato Y, Harada K, Sasaki M, Yoneda N, Lin ZH, Nakanuma Y. Biliary infection may exacerbate biliary cystogenesis through the induction of VEGF in cholangiocytes of the polycystic kidney (PCK) rat. Am. J. Pathol. 2011; 179(6):2845–2854. [PubMed: 22015458]
28. Huwart L, Peeters F, Sinkus R, Annet L, Salameh N, ter Beek LC, Horsmans Y, Van Beers BE. Liver fibrosis: non-invasive assessment with MR elastography. NMR Biomed. 2006; 19(2):173–179. [PubMed: 16521091]
29. Rouviere O, Yin M, Dresner MA, Rossman PJ, Burgart LJ, Fidler JL, Ehman RL. MR elastography of the liver: preliminary results. Radiology. 2006; 240(2):440–448. [PubMed: 16864671]
30. Messroghli DR, Radjenovic A, Kozerke S, Higgins DM, Sivananthan MU, Ridgway JP. Modified Look-Locker inversion recovery (MOLLI) for high-resolution T_1 mapping of the heart. Magn. Reson. Med. 2004; 52(1):141–146. [PubMed: 15236377]
31. Deichmann R, Hahn D, Haase A. Fast T_1 mapping on a whole-body scanner. Magn. Reson. Med. 1999; 42(1):206–209. [PubMed: 10398969]
32. Doyle FH, Pennock JM, Banks LM, Mcdonnell MJ, Bydder GM, Steiner RE, Young IR, Clarke GJ, Pasmore T, Gilderdale DJ. Nuclear magnetic resonance imaging of the liver: initial experience. Am. J. Roentgenol. 1982; 138(2):193–200. [PubMed: 6275694]
33. Bruegel M, Gaa J, Waldt S, Woertler K, Holzapfel K, Kiefer B, Rummeny EJ. Diagnosis of hepatic metastasis: comparison of respiration-triggered diffusion-weighted echo-planar MRI and five T_2-weighted turbo spin-echo sequences. Am. J. Roentgenol. 2008; 191(5):1421–1429. [PubMed: 18941080]
34. Chen JH, Chai JW, Shen WC. Magnetization transfer contrast imaging of liver cirrhosis. Hepatogastroenterology. 1999; 46(29):2872–2877. [PubMed: 10576364]
35. Taouli B, Tolia AJ, Losada M, Babb JS, Chan ES, Bannan MA, Tobias H. Diffusion-weighted MRI for quantification of liver fibrosis: preliminary experience. Am. J. Roentgenol. 2007; 189(4): 799–806. [PubMed: 17885048]

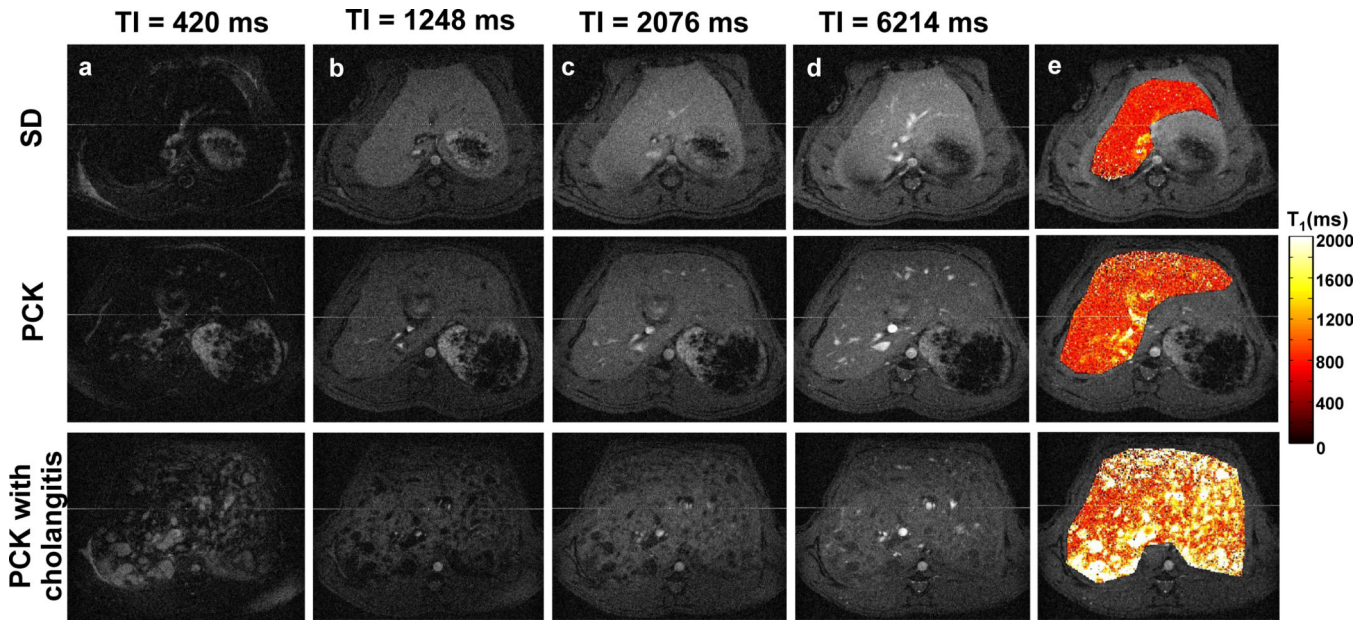

Figure 1.

Representative liver Look-Locker T_1-weighted images (columns a-d, grayscale) and T_1 maps (column e, color scale) from a 3–month-old Sprague-Dawley (SD) control rat (top row) and two age-matched PCK rats (middle and bottom rows). The PCK rat in the bottom row exhibited cholangitis associated with more severe liver disease, which is also observed periodically in ARPKD patients.

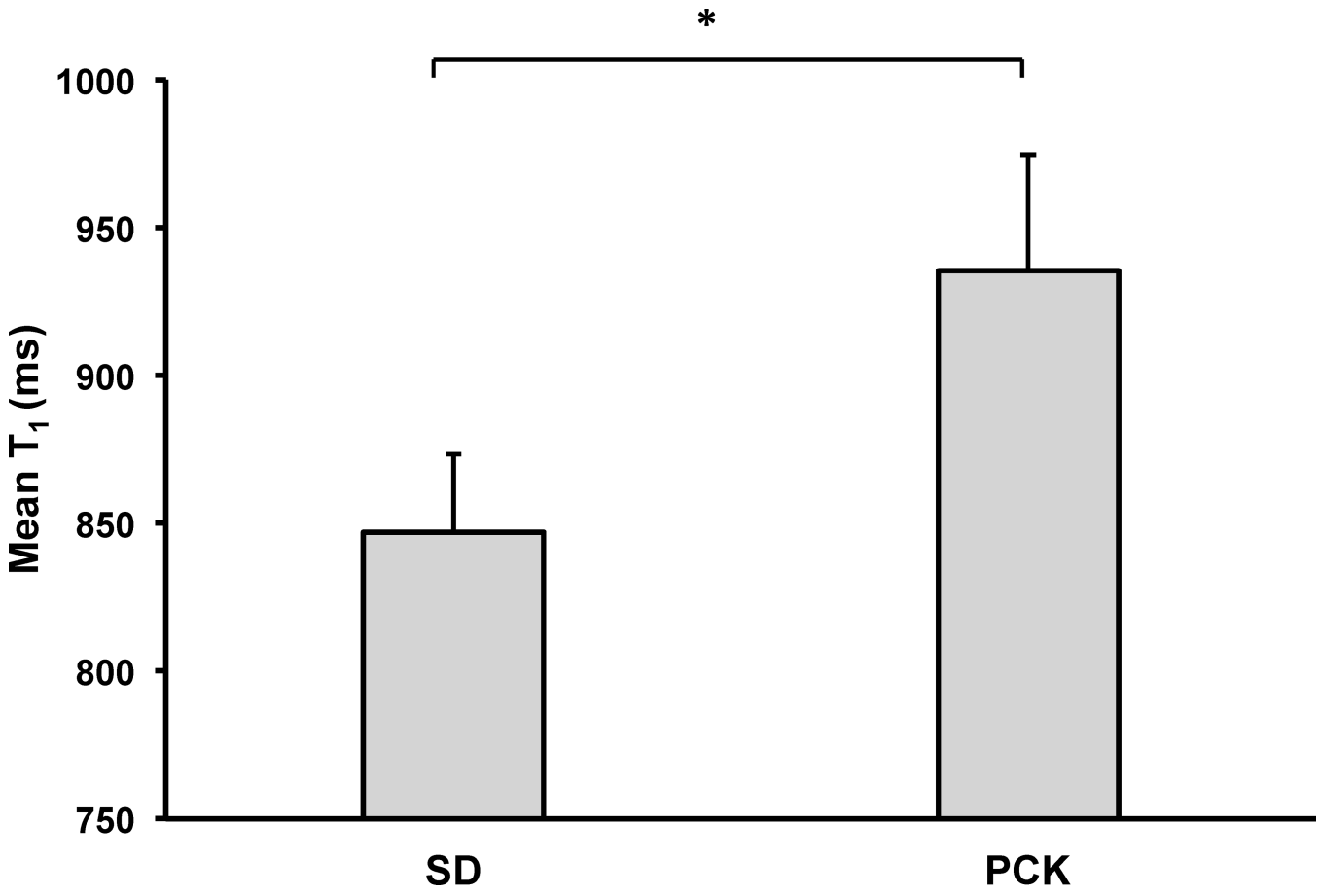

Figure 2.

Plot of mean liver T_1 values for SD (n=6) and PCK (n=4) rats at 3 months of age. The mean T_1 values for the PCK rats were significantly increased in comparison to the SD rats (*p = 0.01). The respective T_1 value for the PCK rat with cholangitis was further increased (n=1, data not shown, mean T_1 = 1413 ms).

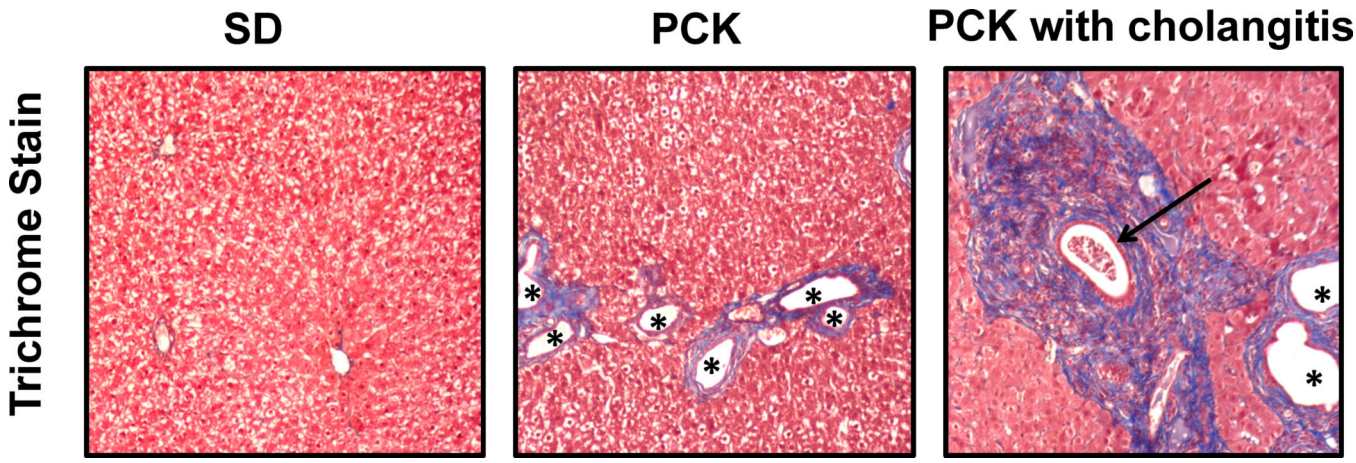

Figure 3.

Photomicrographs (10× original magnification) of SD and PCK rat liver specimens stained with Masson's Trichrome to assess periportal fibrosis (in blue) and biliary dilatation (asterisks *). Note the regions of bile duct proliferation and dilatation as well as increased fibrosis in the PCK rats. Periportal fibrosis is especially pronounced in the rat with cholangitis, in which inflammatory cells are evident within a dilated bile duct (arrow).

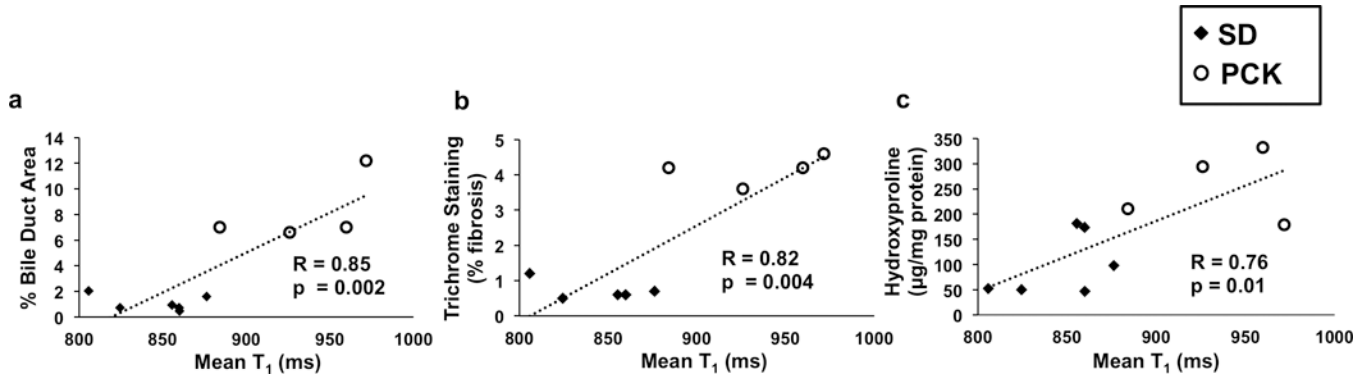

Figure 4.

Comparison of mean hepatic T_1 values for 3-month-old SD rats (black diamonds) and PCK rats (white circles) in: (a) percent bile duct area; (b) percent fibrosis (by Masson's trichrome staining); and (c) biochemical assessments of hepatic hydroxyproline content. All three assessments resulted in significant correlations with mean liver T_1 ($p = 0.002$, 0.004, and 0.01, respectively) suggesting that T_1 assessments are an effective imaging marker for ARPKD liver disease.